

Abiotic controls on periphyton accrual and metabolism in streams: Scaling by dimensionless numbers

Tanya A. Warnaars,¹ Miki Hondzo,¹ and Mary E. Power²

Received 28 February 2006; revised 4 May 2007; accepted 1 June 2007; published 23 August 2007.

[1] Increasingly available high-resolution topographic data from remote sensing motivates the search for topographic features that predict abiotic controls on the distribution and performance of biota. We investigated the extent to which periphyton distribution and stream ecosystem metabolism in a steep upland river drainage network could be predicted from physical conditions that varied with local topography. During the summers of 2003 and 2004, we measured periphyton standing crops and gross primary production and ecosystem respiration rates along a 5 km reach of the South Fork Eel River and six of its tributaries in northern California (39°44'N, 123°39'W). We also measured wetted stream width (B), cross-sectionally averaged stream velocity (U), and streambed photosynthetically active solar radiation (PAR) at each site to investigate the degree to which periphyton abundance and metabolism were related to these indicators, which in turn are partially predictable from models relating environmental parameters to the topographic settings. Dimensional analysis, a technique widely used in the field of fluid mechanics, was used to investigate how biotic and abiotic variables may be interconnected in stream environments. Nondimensional groups of variables were formulated on the basis of our field estimates of chosen biotic and abiotic variables. Periphyton biomass was controlled by $B^{9/5}$, exposure to light $PAR^{1/5}$, nutrient concentration $N^{5/6}$, and inverse stream depth $H^{-5/6}$ and $U^{-1/2}$. The autotrophic-heterotrophic balance, quantified by the gross primary production to ecosystem respiration rate, scaled with the stream aspect ratio $(B/H)^{3/5}$ and Peclet number $Pe = (UB/u_*H)^{3/10}$, where u_* is the shear stress velocity. The scaling relationships were validated against reported field measurements from other geographical areas. The results show nonlinear dependencies among periphyton biomass, stream metabolism, and abiotic variables. These nonlinear relationships point to a need for detailed quantification of biotic and abiotic variables over a range of scales.

Citation: Warnaars, T. A., M. Hondzo, and M. E. Power (2007), Abiotic controls on periphyton accrual and metabolism in streams: Scaling by dimensionless numbers, *Water Resour. Res.*, 43, W08425, doi:10.1029/2006WR005002.

1. Introduction

[2] Abiotic and biotic factors both limit the accrual and metabolism of primary producers, notably photosynthetic organisms, in stream periphyton [Hynes, 1970; Finlay *et al.*, 1999; Dodds and Biggs, 2002; Wellnitz and Rader, 2003; Müllner and Schagerl, 2003; Biggs *et al.*, 2005]. Abiotic controls of periphyton include fluid flow (magnitude and variability) across a range of scales [Biggs *et al.*, 1999a; Clausen and Biggs, 2000; Biggs and Smith, 2002], nutrient supply [Biggs, 2000; Dodds and Biggs, 2002; Opsahl *et al.*, 2003], and photosynthetically active radiation (PAR) [Power, 1984; Biggs *et al.*, 1999b; Trudeau and Rasmussen, 2003; Bernhardt and Likens, 2004; Hillebrand, 2005]. The relationships between these factors and ecological responses

have proven complex, and highly nonlinear. For example, fluid motion can facilitate periphyton accrual by enhancing nutrient uptake and removal of waste compounds [Whitford and Shumacher, 1964; Hondzo and Wang, 2002]. Above certain velocities, however, periphyton becomes detached and exported downstream [Fisher *et al.*, 1982; Biggs *et al.*, 2005]. The inherent high spatial and temporal variability of the diverse abiotic variables that control algae, as well as their strongly nonlinear impacts on organisms and assemblages, make quantifying physical controls of biota across real landscapes extremely challenging.

[3] In channel networks, water motion is responsible for carving out streambeds as well as influencing the distribution of species and their taxonomic composition. Organisms present in streams are subject to an array of fluid flow variables including drag forces, velocity gradients, and associated mass transfer processes [Hart and Finelli, 1999]. Not only do these variables change spatially, as a consequence of changing channel morphology, they also vary temporally. Unless overridden by biotic controls, such as grazing, physical factors influencing growth should partially predict algal biomass. Periphyton in turn is a major control of

¹Saint Anthony Falls Laboratory, Department of Civil Engineering, University of Minnesota, Minneapolis, Minnesota, USA.

²Department of Integrative Biology, University of California, Berkeley, California, USA.

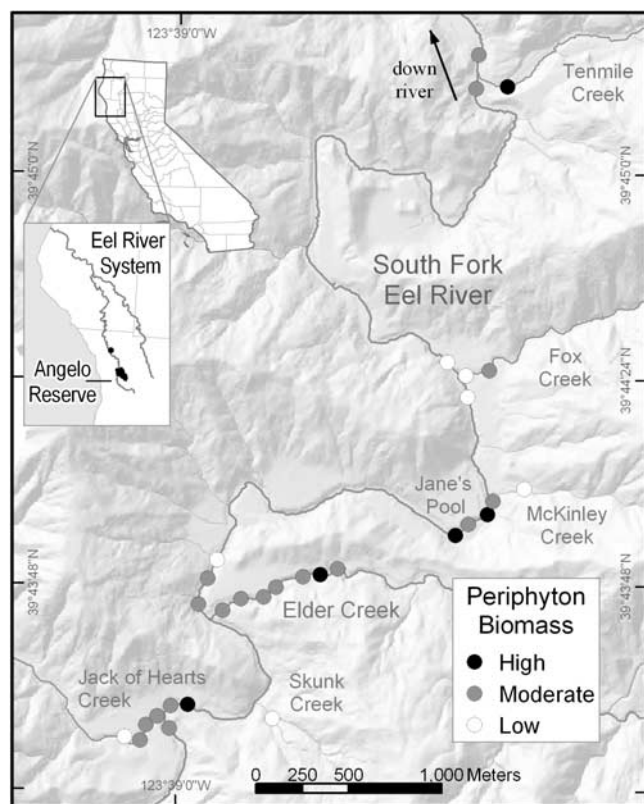


Figure 1. Map of the Angelo Coastal Range Reserve (39°44'N, 123°39'W) indicating sampling locations and periphyton biomass distribution for sampling period 2004 in terms of AFDW where values above 17 g/m² indicate high biomass and values below 1.8 g/m² indicate low biomass estimates.

stream metabolism [Gordon *et al.*, 2004; Mulholland *et al.*, 2005], and consequently disturbances on watershed or stream reach scale not only impacts periphyton accrual, but also stream metabolism as a whole. Algal photosynthetic activity is responsible for reducing the oxygen deficit present in aquatic systems, and maintaining adequate dissolved oxygen (DO) concentrations, which is paramount to sustaining viable lotic ecosystems.

[4] In stream ecosystems, abiotic factors vary over an environmental template [Southwood, 1977] that is shaped both by channel and valley geomorphology and by large riparian vegetation and woody debris [Hynes, 1975; Maser and Sedell, 1994; Gran and Paola, 2001; Tal *et al.*, 2004]. We can now evaluate this template at spatial scales relevant to organisms using advanced remote sensing technologies such as airborne laser swath mapping [Clark *et al.*, 2004; Morris *et al.*, 2005; Dietrich and Perron, 2006]. Motivated by these increasingly available spatial and temporal mapping and sensing technologies [Power *et al.*, 2005], we investigated relationships between landscape position, local abiotic conditions and periphyton biomass, gross primary production (P), ecosystem respiration (R), and autotrophic-heterotrophic balance, quantified by P to R ratio (P/R) in a river drainage network. Field measurements were conducted during summer base flow periods with stable streambed

conditions when abiotic variables affect the supply of light and nutrients available to periphyton. We used dimensionless analysis to investigate scaling relations between periphyton biomass plus stream metabolism and abiotic environmental variables. The method uses knowledge of the dominant parameters to develop functional relationships and identify key parameters governing a functional dependence between biotic and abiotic variables. The power of applying dimensionless analysis was that it acts as a guide for generalizing the complex interaction of how physical, biological and chemical process could be interconnected in stream environments.

2. Materials and Methods

2.1. Study Site

[5] The Angelo Coastal Range Reserve encompasses 5 km of the South Fork of the Eel River and six of its tributaries in Mendocino County, California (Figure 1). The steep upland watershed supports a mixed deciduous and conifer forest, dominated by Douglas fir (*Pseudotsuga menziesii*) and tanoak (*Lithocarpus densiflora*), with redwoods, white alder (*Alnus rhombifolia*) and Oregon ash (*Fraxinus latifolia*) confined largely to the river corridors, and riparian zones. The region's Mediterranean-type climate has an annual precipitation of ~215 cm that falls almost entirely in the winter months [Mast and Clow, 2000]. Stream discharges are high in the winter and decline to stable summer base flows. Consequently, along the main stem South Fork Eel, the forest is generally set back from the edge of the summer inundated channel (10–30 m wide) by cobble bars that are kept open by high flows in the wider (50–100 m) winter active channel. Detailed airborne laser altimetry data were available for the entire watershed (W. E. Dietrich, National Center for Earth-surface Dynamics and National Center for Airborne Laser Mapping, unpublished data, 2007) and were used to quantify elevation, gradients, and drainage areas of channels at sampled sites. During summer base flows, the streams within the Angelo Coast Range Reserve are clear, have high DO concentrations, low to moderate nutrient and dissolved organic carbon concentrations, and high productivity in sunlit areas [Finlay, 2004]. We sampled sites with drainage areas from 0.5 to 275 km² and mean stream slopes from 0.001 to 0.14, which allowed us to investigate a wide range of fluid flow and light conditions associated with contrasting habitat structure (Table 1 and Figure 1).

2.2. In-Stream Measurements: Biomass

[6] Periphyton biomass was assessed in terms of chlorophyll *a* content, ash free dry weight (AFDW) and taxonomic composition. Three samples were collected along cross-stream transects at each sample location (Figure 1) from the left and right banks and the channel centre. Periphyton was scraped off of 8.0 cm² of randomly selected stream substrate. Samples were immediately preserved in Lugol's solution and analyzed later in the laboratory. For AFDW, samples were dried to constant weight at 105°C weighed, then combusting at 500°C for one hour. The ash residue weight was subtracted from dry weight to obtain AFDW measurements. Chlorophyll *a* was determined spectrophotometrically using 90% acetone extraction [American Public

Table 1. List of Streams, Locations, and Average Cross-Sectional Physical, Chemical, and Biological Characteristics During the 2004 Measurements at the Angelo Coast Range Reserve^a

Location Name	Drainage Area, km ²	Stream Slope	Stream Velocity, cm/s	Bank Width, m	Stream Depth, m	Temperature, deg C	pH	PAR, $\mu\text{E}/\text{s}/\text{m}^2$	AFDW, g/m ²	Chlorophyll <i>a</i> , mg/m ²	Nitrate, $\mu\text{g}/\text{L}$	SRP, $\mu\text{g}/\text{L}$
Skunk	0.54	0.137	0.1	1.5	0.15	10.9	-	-	2.30	0.93	2.7	31.5
McKinley	0.58	0.049	0.2	1.8	0.13	12.6	-	-	0.93	0.64	1.1	20.1
Upper Fox	2.72	0.112	(2.1)	(1.6)	(0.26)	(18.0)	(8.0)	(55.1)	(0.99)	(0.70)	(25.0)	(17.9)
Lower Fox	2.74	0.090	2.0 (1.7)	1.5 (1.1)	0.14 (0.31)	13.2 (18.3)	7.8 (7.9)	9.5 (20.2)	2.13 (0.72)	0.46 (0.74)	10.7 (21.2)	22.7 (16.7)
Jack of Hearts (JH)	10.14	0.032	5.7	4.5	0.19	12.3	7.7	3.4	2.32	0.42	1.2	22.7
Upper Ten Mile	140.00	(0.018)	(6.4)	(7.5)	(0.19)	(21.5)	(8.5)	(-)	(6.95)	(5.14)	(5.9)	(8.3)
Lower Ten Mile	140.00	0.070	6.4 (6.4)	15.8 (9.0)	0.35 (0.23)	20.1 (21.5)	8.4 (8.5)	53.2 (22.9)	48.03 (22)	23.04 (6.74)	1.8 (7.3)	15.4 (4.1)
Upper Elder	16.58	0.014	4.8 (4.9)	8.7 (4.0)	0.21 (0.28)	12.3 (17.8)	8.1 (8.1)	143.5 (9.1)	7.58 (1.61)	13.29 (0.93)	1.5 (10.4)	20.5 (18.8)
Lower Elder	16.95	0.029	12.1 (14.1)	4.5 (3.7)	0.27 (0.22)	12.4 (18.0)	7.9 (8.1)	90.7 (51.8)	5.03 (2.48)	5.49 (0.95)	1.4 (8.8)	20.0 (15.5)
South Fork Eel above Jack of Harts	114.44	0.009	16.6	13.2	0.33	14.9	-	-	8.69	6.35	1.6	18.7
South Fork Eel below Jack of Harts	124.81	0.005	50.0	12.3	0.75	14.3	7.8	315.4	41.40	9.50	-	-
South Fork Eel above Elder	125.78	0.003	10.0	15.4	0.45	14.3	7.9	101.1	52.17	9.75	0.5	17.4
South Fork Eel below Elder	142.80	0.003	9.1	11.1	0.32	13.9	7.9	27.3	42.03	11.92	2.7	16.6
South Fork Eel above Jane's Pool	144.83	0.006	3.8 (13.1)	18.5 (7.4)	1.01 (0.19)	15.6 (23.1)	7.9 (8.5)	460.4 (257.3)	18.63 (17.40)	5.68 (27.79)	0.7 (13.6)	16.4 (7.4)
South Fork Eel below Jane's Pool	144.94	0.005	11.8 (14.8)	11.3 (10.6)	0.70 (0.36)	15.8 (23.3)	8.2 (8.4)	210.8 (190.1)	11.18 (12.91)	24.53 (6.70)	1.3 (21.2)	18.7 (7.13)
South Fork Eel at Fox	148.91	0.007	7.8 (10.1)	11.8 (11.5)	0.37 (0.25)	16.4 (23.5)	8.1 (8.5)	(20.2)	1.2 (4.01)	0.55 (2.92)	1.6 (13.6)	20.9 (1.5)
South Fork Eel above Ten Mile	135.04	0.001	4.1	14.4	0.78	18.1	8.2	417.7	9.11	23.66	5.2	16.9
South Fork Eel below Ten Mile	275.51	-	14.0 (11.0)	10.3 (11.1)	0.63 (0.32)	18.8 (21.6)	8.4 (8.6)	379.8 (309.2)	25.26 (3.96)	36.24 (2.29)	5.4 (12.7)	16.1 (5.6)

^aQuantities in parentheses indicate measurements from sampling year 2003.

Health Association (APHA), 1998]. Periphyton producers were identified under 400 \times magnification.

2.3. In-Stream Measurements: Nutrients

[7] Water samples were collected at the same time and place as the periphyton samples. Samples were filtered (Millex-HV with a 0.45 μm pore size) and analyzed for nitrate (NO_3), ammonium, and soluble reactive phosphorus (SRP) concentrations using the Cd reduction, phenate, and ascorbic acid methods (4500 NO_3 -F, 4500 NH_3 -G, 4500 P-G, respectively) [APHA, 1998] on a Lachat QuickChem 8000 flow injection analysis automated ion analyzer (Hach Company, Loveland, Colorado, United States).

2.4. In-Stream Measurements: Abiotic

[8] Stream cross-sectional areas were measured every 10 to 100 m along reaches ranging between 100 to 500 m in length. Cross sectional measurements of the fluid flow and streambed topography were made using a three-dimensional StreamPro acoustic-Doppler current profiler (RD Instruments, San Diego, California, United States), where a minimum of three transects per cross section were performed. In narrow shallow water channels (less than 20 cm deep), vertical point velocity profiles were made, along the cross section, using a two-dimensional flow tracker acoustic-Doppler velocimeter (ADV), Sontek YSI Inc., San Diego, California, United States). For these locations wetted stream width was collected with a measuring tape and every 10 cm along the width the depth was recorded. Hydrolab water quality probes (Data-Sonde 4a, Hach Environmental) were placed on the streambed and used to record the PAR, temperature, pH, and DO concentration at the sampling locations. The data were recorded every 5 min over a 48-hour measuring period.

2.5. Metabolism Calculations

[9] An array of different approaches to estimating stream metabolism exists [Bott, 1996; Mulholland et al., 2001, 2005; Wang et al., 2003; McBride and Chapra, 2005; Webster et al., 2005; Bott et al., 2006; Colangelo, 2007]. The estimation methods are based on the fundamental signature of the DO concentration, as the photosynthetic activity of primary producers releases oxygen. Measuring changes in DO overtime, at a particular stream location, captures the decrease (attributed to respiration) and increase (ascribed to primary producers and gas exchange across the air-water interface) of DO with different water temperatures.

[10] The DO and temperature data we collected enabled calculations for the estimated P (gross primary productivity) and R (ecosystem respiration) rates of the various river reaches [Odum, 1956; Mulholland et al., 2001; Wang et al., 2003]. Algae and other aquatic plants are responsible for P, while R measures the rates of respiration by aquatic plants, algae, fish, invertebrates, and microbes. Volume-based estimations of the metabolic rates were obtained using the "delta method" described by Chapra [1997]. The delta method is based on a mass balance model of diurnal DO measurements and uses stream velocity, reaeration coefficient and a graphical representation of the DO deficit. The reaeration coeffi-

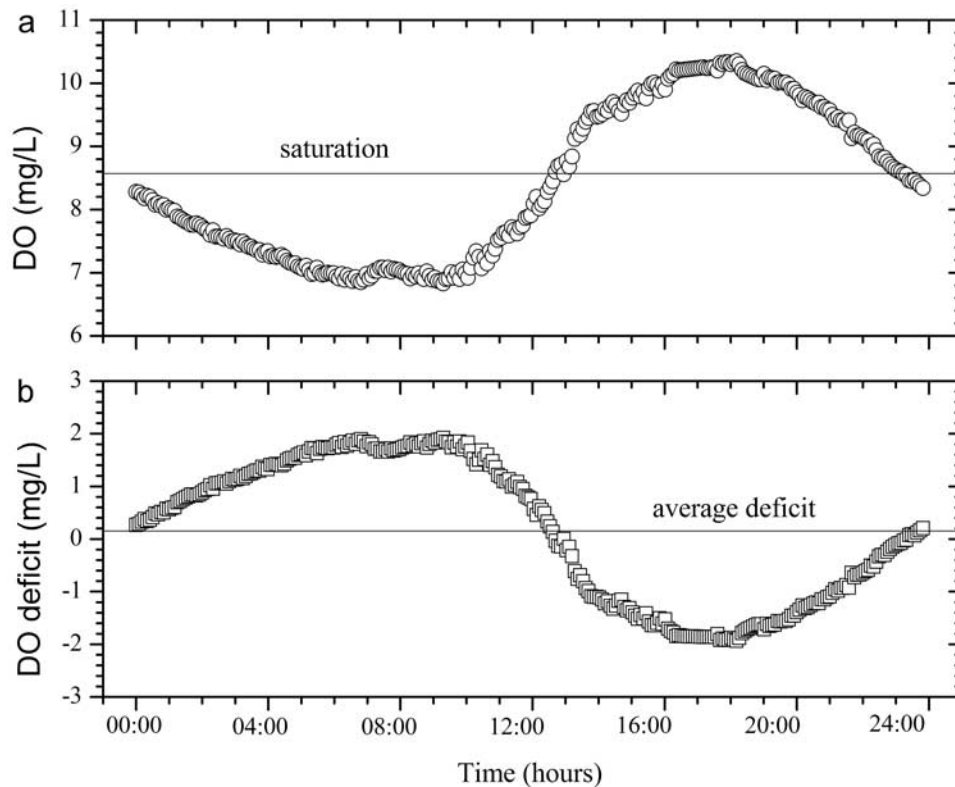


Figure 2. Diurnal profile recorded in the South Fork Eel River at Jane's Pool location of (a) dissolved oxygen concentration and (b) deficit of dissolved oxygen saturation, $D = DO_s - DO$, where DO_s is the DO saturation. U, B, and H were constant during the measuring period.

cient, taken to be independent of photosynthesis and respiration [McBride and Chapra, 2005], was calculated from average stream depth and cross-sectional averaged velocity using the empirical approach of Owens-Edwards-Gibbs [Owens *et al.*, 1964; Chapra, 1997]. This relation was chosen as it was developed and tested in shallow streams (0.12–0.73 m depth) and is recommended at sites with relatively low reaeration rates ($<50 \text{ d}^{-1}$) [Young *et al.*, 2004]. These conditions were closely matched at our field site. In the absence of propane tracer data the selection of this equation was more applicable to our study site than calculating reaeration on the basis of the photoperiod alone [McBride and Chapra, 2005] or the O'Connor-Dobbins formula which is appropriate for deep streams with moderate to low flow [Chapra, 1997; Webster *et al.*, 2005]. Single station diurnal DO measurements provided minimum and maximum DO values, with minimum occurring before solar noon and maximum after solar noon, but before sunset (Figure 2). The diurnal DO profile depicted high variability with minimum at 9 a.m. and maximum around 6 p.m. Since U, H, and B were constant during the diurnal measurements, the DO profile depicts strong biotic signatures during the measurements. Additionally the delta method requires the calculation of the DO deficit, that is the difference between measured and saturated DO concentration (Figure 2). Calculation of the expected saturated DO concentration includes the dependence of oxygen saturation on temperature and pressure (based on exact elevation of the sample site). The difference between measured and expected DO forms the basis for the estimated daily P and R rates.

[11] The effect of groundwater input to streams can bias estimates of P and R [McCutchan *et al.*, 2002]. Groundwater influence and hyporheic flow were negligible at our study site. Vertical hydraulic gradients were only detectable in Elder Creek and ranged between +0.10 and -0.06 in upwelling and downwelling regions, respectively [O'Connor *et al.*, 2006].

[12] The single station diurnal profiles of DO saturation deficit are good indicators of stream P and R rates, and are useful for comparison of metabolism among streams [Mulholland *et al.*, 2005]. The rate of change of DO in a stream is correctly represented by the Stokes total time derivative, which is defined for one-dimensional flow as $\frac{DC_{DO}}{Dt} = \frac{\partial C_{DO}}{\partial t} + U \frac{\partial C_{DO}}{\partial x}$. Single station diurnal DO measurements at a fixed point in the stream provide an estimate for $\frac{\partial C_{DO}}{\partial t}$. These measurements are depicted in the Eulerian reference frame. The corresponding estimates of P and R integrate metabolic activities in the proximity of the measuring point, $\frac{\partial C_{DO}}{\partial x} \approx 0$, where abiotic controls on P and R should be locally measured. The evaluation of spatial gradient, $\frac{\partial C_{DO}}{\partial x}$, requires a two station DO measurements, which consequently makes the estimation of $\frac{DC_{DO}}{Dt}$ possible.

2.6. Dimensional Analysis

[13] Dimensional analysis is a conceptual tool developed in the field of fluid mechanics to understand functional dependencies among different variables that influence a particular process. The purpose of the analysis is to formulate useful dimensionless groups of variables to describe the process and to establish a basis for similarity between the processes at different time and space scales [Potter *et al.*,

Table 2. Variables Used in Dimensionless Analysis and Their Corresponding Units and Dimensions^a

Variable	Symbol	SI Units	Dimensions
Periphyton biomass	C	mg/m ²	M/L ²
Stream velocity	U	m/s	L/T
Stream width	B	m	L
Stream depth	H	m	L
PAR	PAR	J/s/m ²	M/T ³
Medium grain size	D ₅₀	m	L
Grazing rate	G	l/s	1/T
Nutrient concentration	N	mg/L	M/L ³
Photosynthetic rate ^b	P	mg O ₂ /L/s	M/L ³ /T
Respiration rate ^c	R	mg O ₂ /L/s	M/L ³ /T
Shear stress velocity	u*	m ² /s	L ² /T
Specific heat of water	c _p	J/kg/°C	L ² /T ² /K
Stream temperature	T _w	°C	K
Drainage area	A _w	m ²	L ²

^aK is temperature, L is length, M is mass, and T is time. PAR is typically measured in $\mu\text{E}/\text{m}^2/\text{s}$. An approximate conversion for daylight source is to convert $\mu\text{E}/\text{m}^2/\text{s}$ to $\text{J}/\text{s}/\text{m}^2$ dividing $\mu\text{E}/\text{m}^2/\text{s}$ by 4.6 [Biggs, 2005; Townsend and Padovan, 2005].

^bGross primary production.

^cEcosystem respiration.

2002]. Knowledge of the process is required to identify the governing dependent and independent variables and to express a functional relationship with the variables in question. Only by applying data can the generated groupings be given a functional format and provide scaling relationships for the dependent variables.

[14] For example, prior conceptual knowledge allows us to hypothesize that periphyton biomass (C, mass per area (M L^{-2}), Table 2), is dependent on variables such as nutrient concentration (N), cross-sectional averaged stream velocity (U), cross-sectional averaged stream depth (H), wetted bank width (B), medium sediment grain size (D_{50}), PAR, and the rate of loss to grazing (G). Periphyton biomass can be written as a function of these chosen variables

$$C = f_1(U, B, H, \text{PAR}, D_{50}, N, G) \quad (1)$$

where f_1 is an unknown function. All variables outlined in (1) were measured in situ, with the exception of the grazing rate (G). G was derived from grazer exclusion experiments in tributaries with drainage areas spanning the range of 1–20 km² where a correlation has been established between removal rate and drainage area [McNeely and Power, 2007]. An experimental strategy for finding the dependence of periphyton biomass on these variables could be to fix all variables except one (e.g., the velocity) and investigate the dependence of periphyton biomass on the velocity [e.g., Hondzo and Wang, 2002].

[15] Any equation that relates a certain set of variables, such as equation (1), can be written in terms of dimensionless variables. There are several conceptually similar procedures that can be used to determine dimensionless variables; one of the simplest is the Rayleigh method [Brodkey and Hershey, 1988]. If all the selected variables in equation (1) are raised to an as-yet unknown power, multiplied together and placed on the left-hand side of equation (1), then the grouping of variables should be equal to a constant that has no dimensions

$$C^a U^b B^c H^d \text{PAR}^e D_{50}^f N^g, G^h = \text{constant} \quad (2)$$

Equation (2) can be rewritten in terms of corresponding dimensions (Table 2)

$$(\text{ML}^{-2})^a (\text{LT}^{-1})^b (\text{L})^c (\text{L})^d (\text{MT}^{-3})^e \cdot (\text{L})^f (\text{ML}^{-3})^g (\text{T}^{-1})^h = \text{dimensionless} \quad (3)$$

If equation (3) is to have no dimensions on the left-hand side, the sum of a given dimension's power should be zero; therefore

$$\text{M} : a + e + g = 0$$

$$\text{T} : -b - 3e - h = 0 \quad (4)$$

$$\text{L} : -2a + b + c + d + f - 3g = 0$$

There are eight unknowns in equation (4), which correspond to the eight starting variables in equation (1). A key theorem in dimensional analysis, the Buckingham Pi theorem, states that a physically meaningful equation with n physical variables that can be expressed in terms of k independent fundamental physical dimensions, the original expression is equivalent to a set of $p = n - k$ dimensionless groups constructed from the original variables. In our case $n = 8$ and $k = 3$, therefore five dimensionless groups are needed. Equation (4) can be solved in terms of five of the unknowns, we are considering how C^a (i.e., periphyton) is affected, and the variables are written

$$\text{M} : e = -a - g$$

$$\text{T} : b = -3e - h$$

$$\text{L} : c = 2a - b - d - f + 3g$$

$$(\text{substituting } e \text{ and } b \text{ gives : } c = -a + h - d - f) \quad (5)$$

Therefore equation (2) becomes

$$C^a U^{-h+3a+3g} B^{-a+h-d-f} H^d \text{PAR}^{-a-g} D_{50}^f N^g G^h = \text{constant} \quad (6)$$

By grouping variables that share exponents the five dimensionless groups are obtained

$$\left(\frac{C U^3}{B \text{PAR}} \right)^a = f_2 \left[\left(\frac{H}{B} \right)^d, \left(\frac{D_{50}}{B} \right)^f, \left(\frac{N U^3}{\text{PAR}} \right)^g, \left(\frac{G B}{U} \right)^h \right] \quad (7)$$

Equation (7) suggests dimensionless periphyton concentration, i.e., concentration normalized by $(U^3/B/\text{PAR})$, is a function of four dimensionless groups. The function (f_2) is unknown and must be determined using field or laboratory measurements. A physical interpretation of equation (7) is that normalized periphyton concentration is determined by interactions of four dimensionless groups of variables. Dimensionless groups share the important property of dimension independence and therefore the comparison of dimensionless groups under different space scales and timescales is facilitated. The process of dimensional analysis differs to statistical correlation and attempts to attribute cause/effect properties to the variables chosen in the starting analysis (equation (1)).

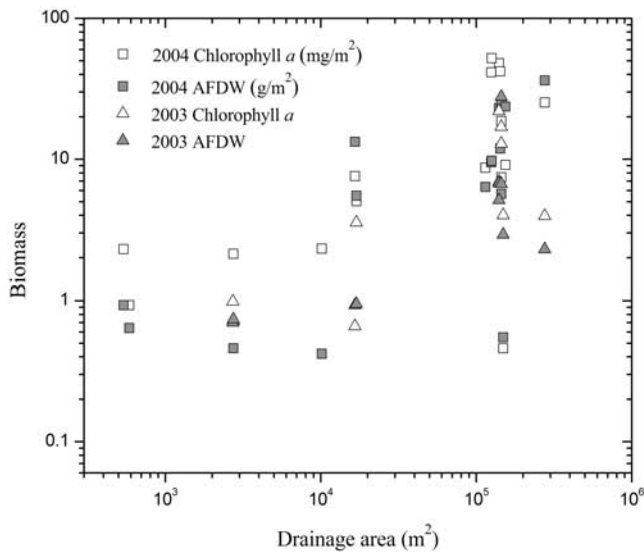


Figure 3. Increasing periphyton biomass measured as chlorophyll *a* and AFDW as a function of drainage area.

[16] Because of the interdependency of periphyton biomass and stream metabolism, dimensionless analysis was also conducted on the P and R rates. For P the chosen influential variables were

$$P = f_3(C, U, B, H, c_p, T_w, PAR, u_*) \quad (8)$$

where $u_* = (g HS)^{0.5}$ is the shear stress velocity, S is the stream slope, c_p is the specific heat of water, and T_w is the water temperature (Table 2). Water temperature is recognized as influencing metabolic rates [Uehlinger *et al.*, 2000; Biggs *et al.*, 1999a] and for unit conformity c_p was included. Nutrient concentrations (notably nitrogen and phosphorus) are known to influence biomass of photosynthetic organisms [Biggs, 2000; Dodds and Biggs, 2002; Opsahl *et al.*, 2003], albeit with time lags; that is, high algal biomass may lower dissolved nutrients in ambient water by uptake, such that an instantaneous measurement may not detect a positive correlation of the two variables. Our periphyton biomass term, C , likely reflects the past availability of nutrients from which the photosynthetic organisms were constructed. From equation (8), five dimensionless groups can be formed

$$\left(\frac{P B^2}{C U}\right)^a = f_4 \left[\left(\frac{B PAR}{C U^3}\right)^b, \left(\frac{c_p T_w}{U^2}\right)^c, \left(\frac{B}{H}\right)^d, \left(\frac{U}{u_*}\right)^e \right] \quad (9)$$

For R the chosen variables considered influential were written as

$$R = f_5(C, A_w, T_w, c_p, U, B, H) \quad (10)$$

where A_w is the drainage area. Four dimensionless groups are possible from equation (10)

$$\left(\frac{R B^2}{C U}\right)^a = f_6 \left[\left(\frac{A_w}{B^2}\right)^b, \left(\frac{B}{H}\right)^c, \left(\frac{c_p T_w}{U^2}\right)^d \right] \quad (11)$$

[17] The P/R ratio was determined by the division of the variables in equation (9) and equation (11) and provided the following expression:

$$\left(\frac{P}{R}\right)^a = f_7 \left[\left(\frac{B^2}{A_w}\right)^b, \left(\frac{B}{H}\right)^c, \left(\frac{c_p T_w}{U^2}\right)^d, \left(\frac{B PAR}{C U^3}\right)^e, \left(\frac{U}{u_*}\right)^f \right] \quad (12)$$

The functional relationships were verified using field measurements collected at the Angelo Coast Range Reserve (Table 1) and are presented in the following sections. For each case the dependent dimensionless groupings (i.e., left side of equations (7) and (12)) were correlated against the log-transformed independent dimensionless groups (i.e., right side of each equation) using the *SPSS Inc.* [2001] multiple linear regression analysis. The independent dimensionless groups that had a significant correlation with the dependent dimensionless group, as measured by the Pearson index, and the groups that were statistically independent were retained for graphical presentation. A best fit functional relationship was set to the data, where the powers for each grouping were obtained from the multiple linear regression analysis.

3. Results

3.1. Field Data: Periphyton Biomass

[18] Periphyton was sampled toward the end of the growing period (late July to early August) in 2003 and earlier before biomass peaked (late May to early June) in 2004. Periphyton in tributaries of the South Fork Eel River: Fox Creek, Elder Creek, and Jack of Hearts Creek, were diatom dominated while most periphyton biomass in the main stem South Fork Eel was made up of filamentous green algae (dominated by *Cladophora glomerata*). The cross-sectional stream averages and variability of the different biomass values and abiotic variables including U , T_w , B , H , S , PAR , SRP , and NO_3 are listed in Table 1. Channel width and depth depicted high spatial heterogeneities with the coefficient of variation 0.6. Periphyton biomass had a 1.2 coefficient of variation. Light availability generally increased downstream with drainage area and stream width, as in most rivers [Vannote *et al.*, 1980]. Both AFDW and chlorophyll *a* measurements indicated periphyton biomass increased with drainage area (Figure 3), though locally the two forms of biomass measurement assisted in data interpretation. The Jack of Hearts Creek tributary had a low biomass based on chlorophyll *a* analysis, but a moderate level of organic matter based on the AFDW, suggesting more organic detritus at this site than elsewhere in the drainage network. Periphyton biomass per unit streambed area, as characterized by AFDW, was unevenly distributed as indicated by high, moderate, and low biomass concentrations in Figure 1. The biomass from chlorophyll *a* content (ranging from 0.46 to 36.24 mg/m²) increased with PAR to the one third power, but was not significantly correlated with U , SRP , and NO_3 (Figure 4).

3.2. Dimensional Analysis: Periphyton Biomass

[19] We used dimensional analysis to ascertain dominant functional relationships between the environmental variables postulated to control periphyton abundance. Each

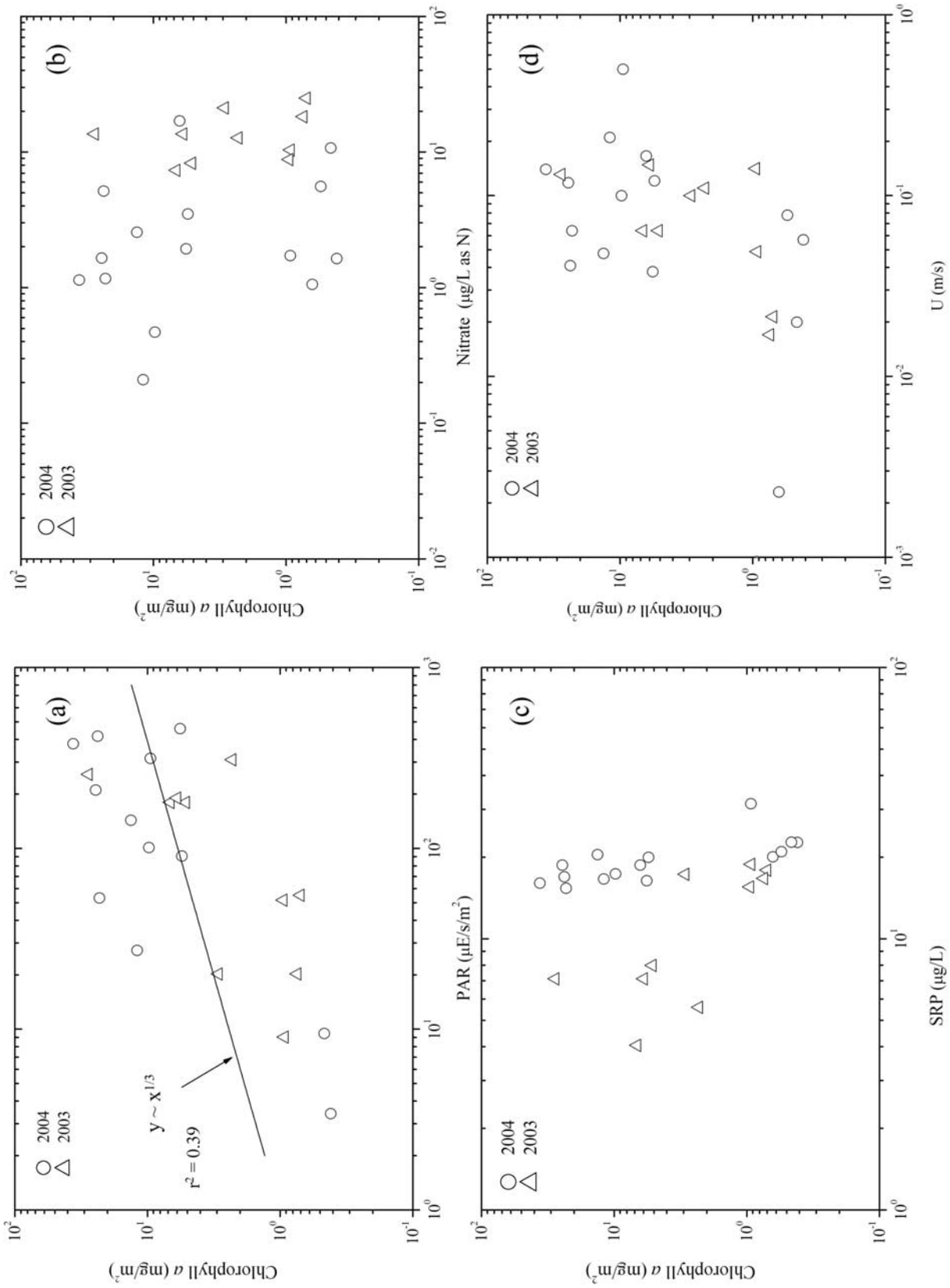


Figure 4. Periphyton biomass in terms of chlorophyll *a* concentration as a function of (a) daily average photosynthetically active radiation (PAR), (b) nitrate concentration (NO_3), (c) soluble reactive phosphorus concentration (SRP), and (d) cross-sectional averaged stream velocity (U).

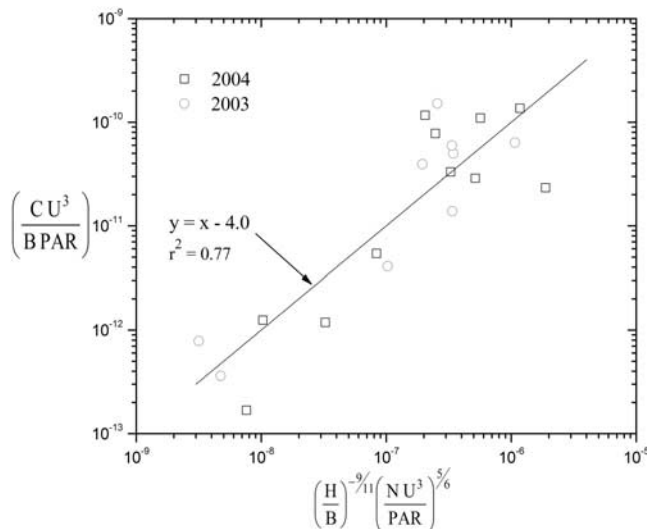


Figure 5. Scaling functional relationship for periphyton biomass. The dimensionless grouping is $(CU^3/B PAR) = 10^{-4}(H/B)^{-9/11}(NU^3/PAR)^{5/6}$. Nutrient concentration (N) is based on SRP, and periphyton biomass (C) is in terms of chlorophyll *a* content.

dimensionless grouping from equation (7) was log transformed and multiple linear regression analysis was performed on the data set. Two dimensionless groups were significantly correlated with the dependent dimensionless group, and were statistically independent from each other. The highest correlation was estimated between $(\frac{CU^3}{B PAR})$ and $(\frac{NU^3}{PAR})$ with the Pearson's $r = 0.84$ ($p \leq 0.01$). The correlation between $(\frac{CU^3}{B PAR})$ and $(\frac{H}{B})$ was $r = -0.54$ ($p \leq 0.05$). The dimensionless groups that were not significantly correlated with the dependent group were excluded from the analysis. Aquatic grazing rates were excluded because they are highly variable both seasonally and spatially throughout the basin area [McNeely, 2004], and the uncertainty of estimating G eliminated the term (GB/U) from the analysis. Therefore our relationships pertain to the residual periphyton biomass (and metabolic activity) that remains after losses to grazers. The functional format of equation (7) with the powers for each dimensionless group obtained by the multiple regression analysis was

$$\left(\frac{C U^3}{B PAR}\right) = 10^{-4} \left(\frac{H}{B}\right)^{-9/11} \left(\frac{N U^3}{PAR}\right)^{5/6} \quad (13)$$

A functional dependence between $(\frac{CU^3}{B PAR})$ versus $(\frac{H}{B})^{-9/11}(\frac{NU^3}{PAR})^{5/6}$ is depicted in Figure 5. The proposed functional dependence explained 77% of the variability in the data. Periphyton biomass, C (measured as chlorophyll *a*), equals

$$C = 10^{-4} \left(\frac{B PAR}{U^3}\right) \left(\frac{H}{B}\right)^{-9/11} \left(\frac{N U^3}{PAR}\right)^{5/6} \quad (14)$$

From (14) the biomass scaled as

$$C \sim \frac{B^{5/6} PAR^{1/6} N^{5/6}}{U^{1/2} H^{5/6}} \quad (15)$$

[20] Compilation of the powers to which each variable was raised provided the above expression and implied chlorophyll *a* concentration scaled to $B^{9/5}$, $PAR^{1/5}$, $N^{5/6}$, the inverse of stream U to the 1/2, and the inverse of H to the 5/6. Both SRP and NO_3 measurements were examined as possible nutrient indicators in the functional format of equation (7). Regression analysis revealed SRP concentrations ($r^2 = 0.77$) better depicted variability of periphyton biomass than NO_3 ($r^2 = 0.63$); consequently SRP measurements were used in generating Figure 5.

3.3. Field Data: Metabolism

[21] Stream metabolism (P and R) increased nonlinearly with drainage area (Figure 6). Sampling was conducted at different stages of the growing season in 2003 and 2004, resulting in differing metabolism measurements for similar drainage areas. The low chlorophyll *a* measurement at Jack of Hearts Creek, corresponded with a low gross primary productivity estimate. The P/R ratio was generally less than one, which could indicate either heterotrophy with significant organic matter inputs from the watershed, or the decomposition of autochthonous (algal) biomass generated earlier in the season. Observations of high algal biomass, and the lack of conspicuous terrestrial litter accumulations, supported the latter interpretation for the main stem channel P/R ratios.

3.4. Dimensional Analysis: Metabolism

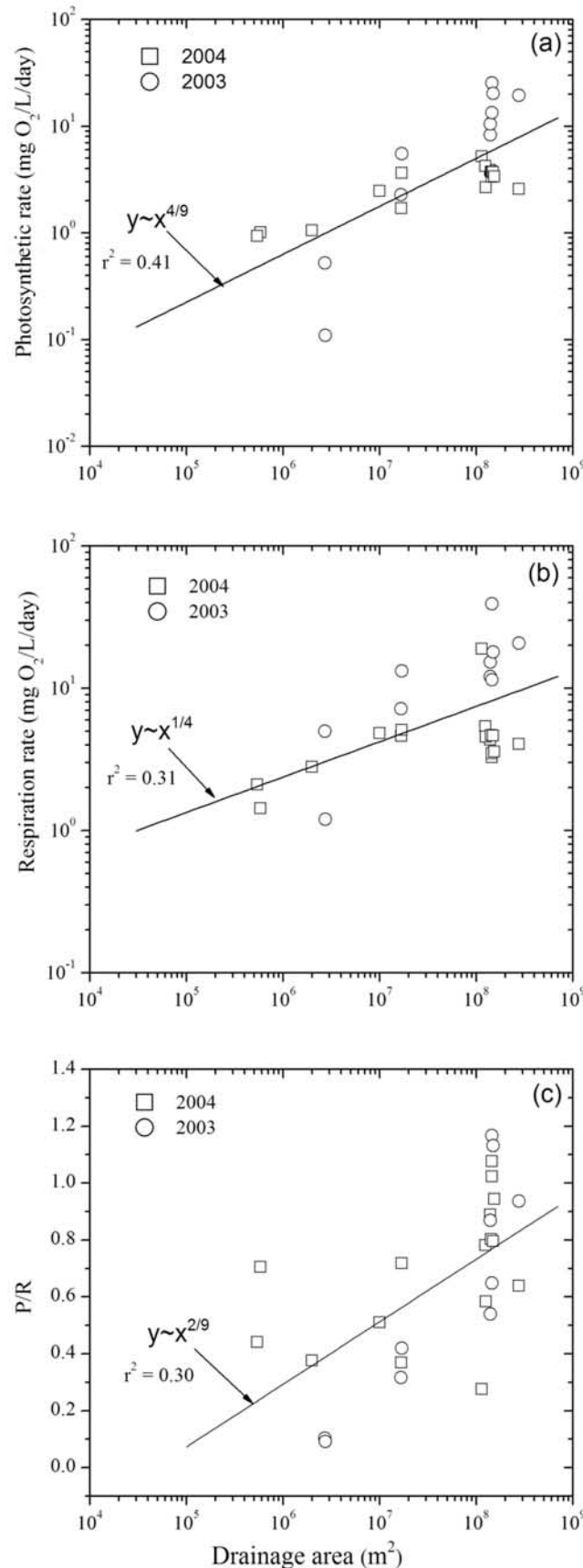
[22] The field estimates of P/R ratios were applied to the proposed dimensionless groupings of equation (12). The highest correlation was estimated between P/R and B/H dimensionless group with the Pearson's $r = 0.77$ ($p \leq 0.01$). The correlation between P/R and U/u_* was $r = 0.64$ ($p \leq 0.01$). The functional format of P/R versus B/H and U/u_* was obtained by multiple regression analysis (Figure 7). The proposed functional dependence explained 62% of the variability in the data with the following relationship

$$\frac{P}{R} = 10^{-1} \left(\frac{B}{H}\right)^{3/5} \left(\frac{U}{u_*}\right)^{1/5} \quad (16)$$

Equation (16) was rewritten and simplified to

$$\frac{P}{R} \sim \left(\frac{B}{H}\right)^{3/5} \left(\frac{U B}{u_* H}\right)^{1/5} \sim \left(\frac{B}{H}\right)^{7/5} Pe^{1/5} \quad (17)$$

where $Pe = \frac{UB}{u_* H}$ is the Peclet number. This dimensionless number represents the ratio of net oxygen transport by advective fluid flow over a characteristic length scale, B, to dispersive transport of oxygen across the channel cross section ($\sim u_* H$). This scaling revealed stream aspect ratio (B/H), which also can be interpreted as a cross-sectional "shape" coefficient, and the corresponding ecosystem Peclet number to be significant abiotic controls in determining the dominance of heterotrophy or autotrophy of a stream ecosystem. Indeed Biggs *et al.* [2005] describe a switch from heterotrophy to autotrophy in the Taieri River (South Island, New Zealand) during periods of low flow when reductions in bed disturbances were observed. In studying the Daly River, Townsend and Padovan [2005] found maximum biomass of *Spirogyra* filaments was limited by shear stress velocity that caused sloughing.



Webster *et al.* [2005] also studied the heterotrophic Daly River and showed that photosynthesis increased steadily at the end of the high-flow period. The importance of channel form and hydraulic conditions on river ecosystem metabolism are known [Uehlinger *et al.*, 2000; Petts, 2000; Mulholland *et al.*, 2001; Biggs *et al.*, 2005], and equation (17) provides a scaling relationship of the drivers governing the balance between autotrophic and heterotrophic processes. Stream aspect ratio and Peclet number propose a scaling relationship for our chosen influential abiotic variables.

3.5. Comparison With Other Studies

[23] Four studies [Biggs *et al.*, 1999a; Uehlinger *et al.*, 2000; Mulholland *et al.*, 2001; Wang *et al.*, 2003] were selected to validate the scaling of proposed functional relationships. All three studies investigated the P and R rates of a variety of streams and rivers. Wang *et al.* [2003] sampled two rivers in Indiana (United States) from July to September. Mulholland *et al.* [2001] had eight study sites in North America covering a diverse set of physical, chemical and biological conditions (e.g., desert to temperate streams). Biggs *et al.* [1999a] conducted their study on the South Island of New Zealand. Overall, these studies represent a wide range of latitudes, climates regimes, drainage areas, and ecosystems.

[24] Mulholland *et al.* [2001] reported periphyton biomass (AFDW) in streams distributed over a large geographic range where they are exposed to a variety of climatic conditions. These data (Figure 8) are well fit by the scaling relationship proposed by equation (13), which was derived from our data on Eel River watershed conditions and periphyton concentrations. The scaling exponents remained unchanged while the multiplying coefficient was changed to reflect conversion between biomass concentration quantified by chlorophyll *a* content (Figure 5) versus biomass concentration quantified by AFDW (Figure 8).

[25] Data on P and R rates from these four studies plotted reasonably well with data from our study proposed by equation (17) (Figure 9). The scaling of P/R ratio corroborated with the reported measurements. The groupings provided the following functional relationship:

$$\frac{P}{R} = 10^{-1.3} \left[\left(\frac{B}{H} \right)^{2/5} \left(\frac{U B}{u_* H} \right)^{1/5} \right]^{3/2} \sim \left(\frac{B}{H} \right)^{3/5} P_c^{3/10} \quad (18)$$

These other studies encompassed a wider range of field conditions. When scaled according to the proposed groups, however, the best fit functional relationship matches the data estimated in this study.

4. Discussion

4.1. Periphyton Biomass

[26] Periphyton distribution on the spatial map (Figure 1) revealed only a few locations with high biomass concen-

Figure 6. Stream metabolism functional dependence on contributing watershed area in terms of average (a) gross primary production (P), (b) ecosystem respiration (R), and (c) autotrophic-heterotrophic balance (P/R ratio).

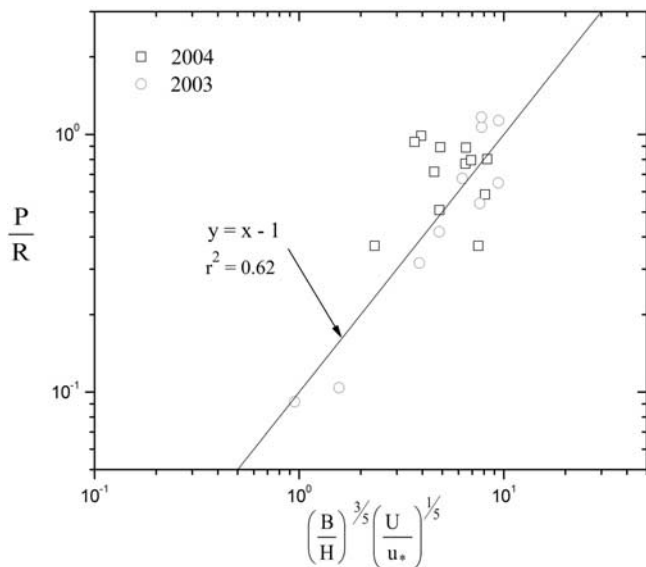


Figure 7. Autotrophic-heterotrophic balance quantified by P to R ratio versus abiotic dimensionless groups.

trations (measured as AFDW). Because of the variation in channel topography and stream hydraulics at sample locations a single controlling variable was not identified (Figure 4). From previous studies [Biggs *et al.*, 1999b, 1998] it is apparent that fluid flow, light levels and nutrients are all important factors influencing periphyton biomass accumulation. The relative strengths of these parameters in controlling periphyton biomass have been difficult to quantify.

Dimensional analysis initially gives equal weighting to each physical variable on which biotic responses depend. Field data are then applied to determine the strength of a given variable listed in the dimensional groupings. It was necessary to make certain assumptions, particularly the omission of the grazing rate. Herbivory is a complex parameter varying temporally for each location, hence the term (GB/U) was not used in developing scaling relationships and we concentrated on abiotic parameters. Therefore our empirical predictions, based only on immediate physical conditions, will underestimate periphyton biomass that would accrue without losses to grazers, particularly in locations with intense grazing activity.

[27] Individual variables, with the exception of PAR, were uncorrelated with periphyton biomass (measured as chlorophyll *a*) (Figure 4). Grouping these variables using dimensionless expressions provided more predictive power than PAR alone (Figure 5), because the independent variables of Figure 5 include PAR plus nutrients, stream morphology and fluid flow velocity as mechanisms controlling periphyton biomass (measured as chlorophyll *a*). The scaling relationship for biomass (equation (15)) indicated increased stream width is linked to increased periphyton biomass. Bank width is correlated to light levels as wider channels are less shaded by riparian vegetation. Rounick and Gregory [1981] studied eight locations and found open sites supported higher periphyton, in terms of chlorophyll *a*, than shaded sites. Canopy cover at the Angelo Coast Range Reserve ranged from 39.0% (South Fork Eel) to 97.0% (Fox) closed [Finlay, 2003]. While increasing light levels facilitates photosynthesis, extreme levels damages the pho-

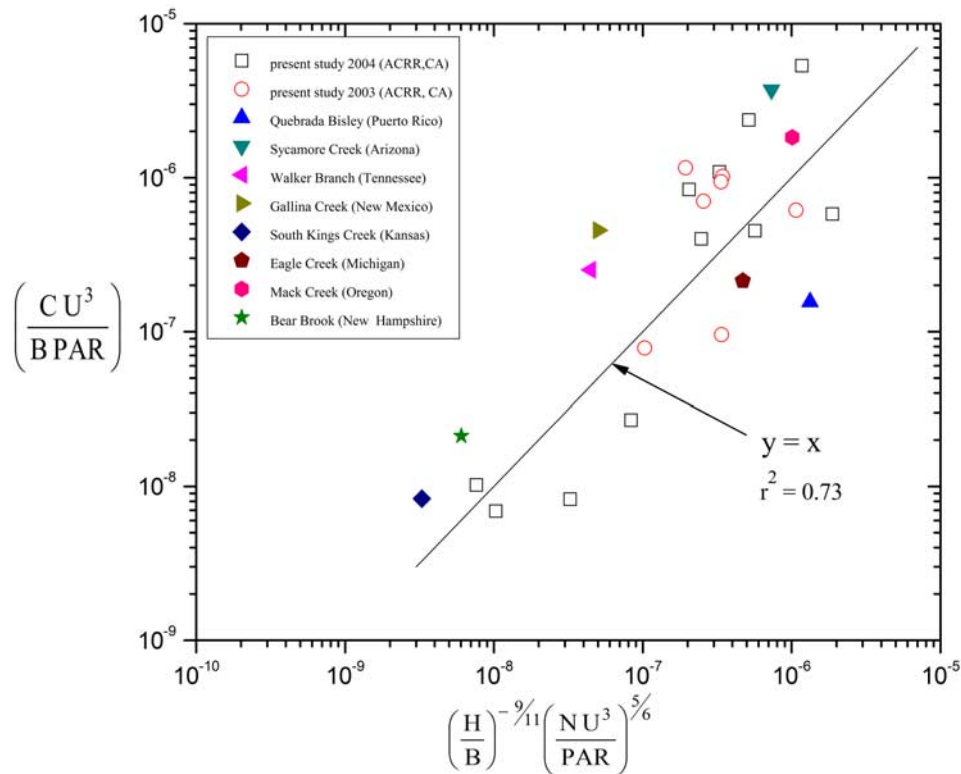


Figure 8. Comparison of present study with other studies [Mulholland *et al.*, 2001] for periphyton biomass (C expressed as AFDW) versus abiotic dimensionless groups of abiotic predictor variables, where ACRR refers to the Angelo Coastal Range Reserve.

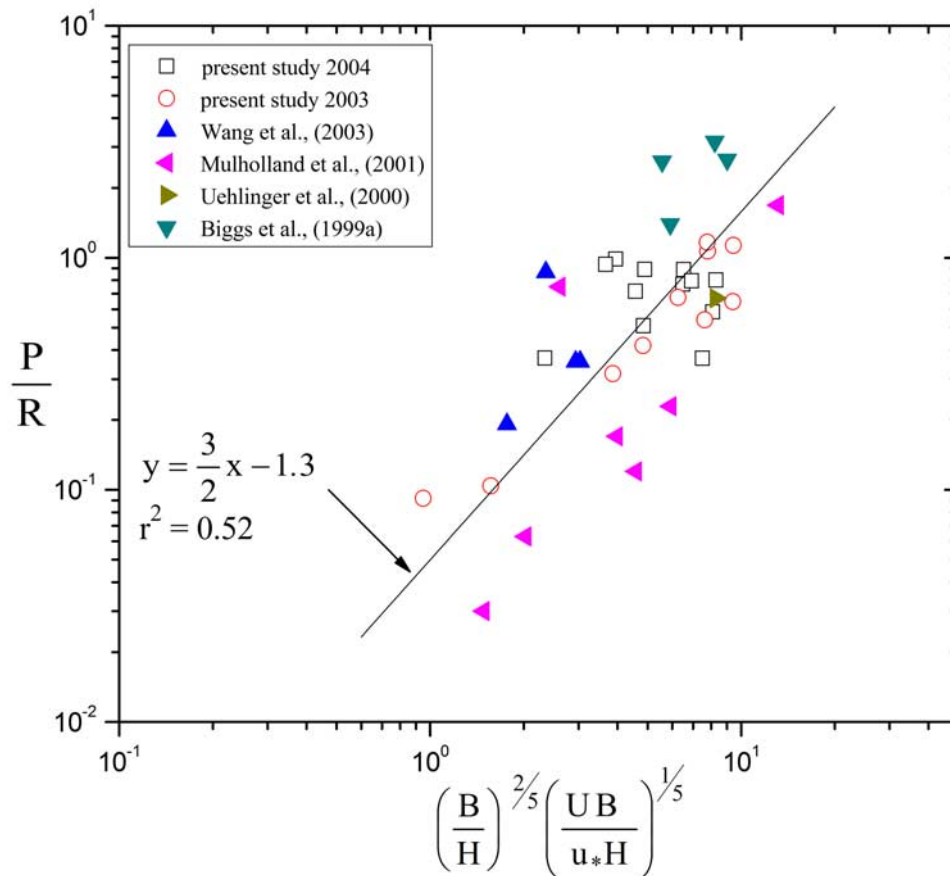


Figure 9. Comparison of present study with studies of net ecosystem production quantified by P to R ratio versus dimensionless abiotic groups.

tosynthetic apparatus [Buchanan *et al.*, 2000] and this could be one explanation for C scaling to PAR to the one fifth power, yet to the square of average stream width. Stream width, in forested canopy covered streams, can be interpreted as a determinant of PAR availability.

[28] Periphyton biomass depended on reciprocal stream average velocity, suggesting that high U values and associated high bed shear stresses were not favorable to biomass accrual. This is coupled to the fundamentals of periphyton being a community of organisms attached to a substrate on the streambed. The beneficial effects of currents, notably increased mass transfer [Opsahl *et al.*, 2003], applied early in the growth season when periphyton was in a more active growth phase. Strong stream fluid flow velocities heighten the risk of periphyton sloughing. With increasing water depth light is attenuated and may explain why C scaled with reciprocal stream depth.

4.2. Stream Metabolism

[29] Gross primary productivity (P) and ecosystem respiration (R) were estimated from single station measurements of diurnal DO concentrations, and in general 2004 had a lower P value than 2003. Biggs *et al.* [1999a] also reported a seasonal difference where the summer maximum photosynthetic rate (P_{max}) was seven times greater than the spring P_{max} , and found that P_{max} also increased with temperature. Temperature may also have played a role in our study, as on average in 2004 water temperature was 5°C cooler than

2003. This year-to-year variation was apparent from P/R ratios where values for a given drainage area differed depending on the measurement date (Figure 6c).

[30] Scaling of P/R showed B, H, and Peclet number primarily influenced stream metabolism. Bank width strongly influenced P, not surprising as in situ primary production is greater for open canopy as compared to closed canopy locations [Allan, 1995; Mulholland *et al.*, 2001]. This exposure facilitates the development of large periphytic mats that consume and produce oxygen, accounting for the P/R ratio scaling with B. Streams of the Angelo Coastal Range Reserve flow over bedrock, and have limited hyporheic zones [O'Connor *et al.*, 2006]; therefore transient storage was accounted for indirectly through B, H and U. Increased u_* exposes periphyton communities to increased drag leading to biomass removal, therefore it is an important parameter to include. Indeed, Biggs and Stokseth [1996] report increased velocity negatively impacted the periphyton community, as increased shear stress increased the export rate of organic material. Townsend and Padovan [2005] state drag on filaments of periphyton exceeded tensile strength and led to removal. The P/R ratio, based on dimensionless analysis, provided a tool for comparison with other studies. Furthermore the relationship was used to develop a Peclet number based on advective and dispersive conditions as a control of the P/R ratio (Figure 9). Application of our field measurements to dimensional analysis has revealed scaling relationships and has provided a means

to estimate the autotrophy and heterotrophy of river systems from different geographical regions.

5. Conclusions

[31] Dimensional analysis revealed the form of functional dependencies between abiotic variables and periphyton abundance and activity. Periphyton distribution and stream ecosystem metabolism were measured in the forested upper watershed of the South Fork Eel River basin in northern California during a time window near the seasonal peak of algal biomass accrual. Our measurements did not account for losses to grazers, which can be significant in this system [Power, 1990; Wootton *et al.*, 1996]. As such, our predictive relationships probably underestimate the accrual that could occur at sites, where only abiotic factors are limiting. Periphyton biomass, gross primary production rate, and ecosystem respiration rate, were controlled by local abiotic variables including stream hydraulics, photosynthetically active radiation, and nutrient concentrations. These abiotic controls were spatially variable, and their relationships with the periphyton biomass and metabolism in streams were highly nonlinear.

[32] Periphyton biomass throughout the drainage network we studied was empirically predicted by the dimensionless grouped variables we generated, including those related to stream hydraulics ($B^{5/6}$, $U^{-1/2}$, $H^{-5/6}$); exposure to light $PAR^{1/5}$; and soluble reactive phosphorus concentration $N^{5/6}$. The proposed scaling relation agreed with measurements in other streams representing a large geographic range (Figure 8). A multiple regression analysis on the comparison of factors predicting stream metabolism revealed the availability of PAR, extent of transient storage zones (through U, B, H), and u_* as control variables [Petts, 2000; Mulholland *et al.*, 2001]. Our results support these findings, provide scaling exponents (based on our field measurements) for the selected control abiotic variables, and emphasize the importance of local stream hydraulic conditions.

[33] The autotrophic-heterotrophic balance, quantified by P to R ratios, was less than one in most of our study reaches. If this result were to hold over the course of an entire year, it could indicate allochthonous contributions to ecosystem respiration. Given the short time course of our summertime measurements, however, $P/R < 1$ was more likely an indication of decomposition of algal biomass fixed earlier in the season, at least in the productive main stem channels. Spatial variation in P/R ratio was empirically predictable from local stream hydraulic conditions (Figure 9) and this variability was also documented in other studies [Biggs *et al.*, 1999a; Uehlinger *et al.*, 2000; Mulholland *et al.*, 2001; Wang *et al.*, 2003]. Stream aspect ratio and ecosystem Peclet number (equation (18)) are proposed as simple scaling indicators of autotrophic-heterotrophic balance in streams (Figure 9). We have demonstrated, with measurements collected at the Angelo Coastal Range Reserve, possible interconnections between physical, biological and chemical processes in stream environments. It is important not to lose sight of the impact of method selection on specific scaling relationships. Our dimensional analysis may provide a guide for future work in generalizing the bio-complexities of stream ecosystem processes.

[34] **Acknowledgments.** This work is supported by the National Center for Earth-Surface Dynamics (NCED), a Science and Technology Center funded by the Office of Integrative Activities of the National Science Foundation (NSF) (under agreement EAR-0120914). We would like to thank Ben O'Connor for providing nitrate and SRP data and W. E. Dietrich for providing airborne laser swath mapping data for the site through the NSF National Center for Airborne Laser Mapping. Map of the Angelo Coastal Range Reserve indicating sampling locations and periphyton biomass distribution (Figure 1) was unconditionally provided by Collin Bode, University of California, Berkeley. We are grateful to the University of California Natural Reserve System and Peter Steel, Resident Director, for maintaining the Angelo Coast Range Reserve as a protected site for research.

References

- Allan, D. (1995), *Stream Ecology Structure and Function of Running Waters*, CRC Press, Boca Raton, Fla.
- American Public Health Association (APHA) (1998), *Standard Methods for Examination of Water and Wastewater*, 20th ed., Washington, D. C.
- Bernhardt, E. S., and G. E. Likens (2004), Controls on periphyton biomass in heterotrophic streams, *Freshwater Biol.*, 49, 14–27.
- Biggs, B. J. F. (2000), Eutrophication of streams and rivers: Dissolved nutrient-chlorophyll relationships for benthic algae, *J. N. Am. Benthol. Soc.*, 19, 17–31.
- Biggs, B. J. F., and R. A. Smith (2002), Taxonomic richness of stream benthic algae: Effects of flood disturbance and nutrients, *Limnol. Oceanogr.*, 47, 1175–1186.
- Biggs, B. J., and S. Stokseth (1996), Hydraulic habitat suitability for periphyton in rivers, *Reg. Rivers Res. Manage.*, 12, 251–261.
- Biggs, B. J., D. G. Goring, and V. I. Nikora (1998), Subsidy and stress responses of stream periphyton to gradients in water velocity as a function of community growth form, *J. Phycol.*, 34, 598–607.
- Biggs, B. J. F., R. A. Smith, and M. Duncan (1999a), Velocity and sediment disturbance of periphyton in headwater streams: Biomass and metabolism, *J. N. Am. Benthol. Soc.*, 18, 222–241.
- Biggs, B. J. F., N. C. Tuchman, R. L. Lowe, and R. J. Stevenson (1999b), Resource stress alters hydrological disturbance effects in a stream periphyton community, *Oikos*, 8, 95–108.
- Biggs, B. J. F., V. I. Nikora, and T. H. Snelder (2005), Linking scales of flow variability to lotic ecosystem structure and function, *River Res. Appl.*, 21, 283–298.
- Bott, T. L. (1996), Primary productivity and community respiration, in *Methods in Stream Ecology*, edited by F. R. Hauer and G. A. Lamberti, pp. 533–556, Elsevier, New York.
- Bott, T. L., J. D. Newbold, and D. B. Arscott (2006), Ecosystem metabolism in Piedmont streams: Reach geomorphology modulates the influence of riparian vegetation, *Ecosystems*, 9, 398–421.
- Brodkey, R. S., and H. C. Hershey (1988), *Transport Phenomena: A Unified Approach*, 847 pp., McGraw-Hill, New York.
- Buchanan, B. B., W. Gruissem, and R. L. Jones (2000), *Biochemistry and Molecular Biology of Plants*, Am. Soc. of Plant Physiol., Rockville, Md.
- Chapra, S. C. (1997), *Surface Water Quality Modelling*, 844 pp., McGraw-Hill, New York.
- Clark, M. L., D. B. Clark, and D. A. Roberts (2004), Small-footprint LIDAR estimation of sub-canopy elevation and tree height in a tropical rain forest landscape, *Remote Sens. Environ.*, 91, 68–89.
- Clausen, B., and B. J. F. Biggs (2000), Flow variables for ecological studies in temperate streams: Grouping based on covariance, *J. Hydrol.*, 237, 184–197.
- Colangelo, D. J. (2007), Response of river metabolism to restoration of flow in the Kissimmee River, Florida, U.S.A., *Freshwater Biol.*, 52, 459–470.
- Dietrich, W. E., and J. T. Perron (2006), The search for a topographic signature of life, *Nature*, 439, 411–418.
- Dodds, W. K., and B. J. F. Biggs (2002), Water velocity attenuation by stream periphyton and macrophytes in relation to growth form and architecture, *J. N. Am. Benthol. Soc.*, 21, 2–15.
- Finlay, J. C. (2003), Controls of streamwater dissolved inorganic carbon dynamics in a forested watershed, *Biogeochemistry*, 62, 231–252.
- Finlay, J. C. (2004), Patterns and controls of lotic algal stable carbon isotope ratios, *Limnol. Oceanogr.*, 49, 850–861.
- Finlay, J. C., M. E. Power, and G. Cabana (1999), Effects of water velocity on algal carbon isotope ratios: Implications for river food web studies, *Limnol. Oceanogr.*, 44, 1198–1203.
- Fisher, S. G., L. J. Gray, N. B. Grimm, and D. E. Busch (1982), Temporal succession in a desert stream ecosystem following flash flooding, *Ecol. Monogr.*, 52, 93–110.

- Gordon, N. D., T. A. McMahon, B. L. Finlayson, C. J. Gippel, and J. R. Nathan (2004), *Stream Hydrology: An Introduction for Ecologists*, John Wiley, Hoboken, N. J.
- Gran, K., and C. Paola (2001), Riparian vegetation controls on braided stream dynamics, *Water Resour. Res.*, *37*, 3275–3283.
- Hart, D. D., and C. M. Finelli (1999), Physical-biological coupling in streams: The pervasive effects of flow on benthic organisms, *Annu. Rev. Ecol. Syst.*, *30*, 363–395.
- Hillebrand, H. (2005), Light regime and consumer control of autotrophic biomass, *J. Ecol.*, *93*, 758–769.
- Hondzo, M., and H. Wang (2002), Effects of turbulence on growth and metabolism of periphyton in a laboratory flume, *Water Resour. Res.*, *38*(12), 1277, doi:10.1029/2002WR001409.
- Hynes, H. B. N. (1970), *The Ecology of Running Waters*, Univ. of Toronto Press, Toronto, Ont., Canada.
- Hynes, H. B. N. (1975), The stream and its valley, *Int. Ver. Theor. Angew. Limnol.*, *19*, 1–15.
- Maser, C., and J. R. Sedell (1994), *From the Forest to the Sea: The Ecology of Wood in Streams, Rivers, Estuaries, and Oceans*, St. Lucie, Delray Beach, Fla.
- Mast, M. A., and D. W. Clow (2000), Environmental characteristics and water-quality of Hydrologic Benchmark Network stations in the western United States, *U.S. Geol. Surv. Circ.*, *1173-d*.
- McBride, G. B., and S. C. Chapra (2000), Rapid calculation of oxygen in streams: Approximate delta method, *J. Environ. Eng.*, *3*, 336–342.
- McCutchan, J. H., J. F. Saunders, W. M. Lewis, and M. G. Hayden (2002), Effects of groundwater flux on open-channel estimates of stream metabolism, *Limnol. Oceanogr.*, *47*, 321–324.
- McNeely, F. C. (2004), Herbivore responses to stream size gradients in a northern Californian watershed, Ph.D. dissertation, Univ. of Calif., Berkeley.
- McNeely, F. C., and M. E. Power (2007), Spatial variation in caddis fly grazing within a northern California watershed, *Ecology*, in press.
- Morris, J. T., D. Porter, M. Neet, P. A. Noble, L. Schmidt, L. A. Lapine, and J. R. Jensen (2005), Integrating LIDAR elevation data, multi-spectral imagery and neural network modelling for marsh characterization, *Int. J. Remote Sens.*, *26*, 5221–5234.
- Mulholland, P. J., et al. (2001), Inter-biome comparison of factors controlling stream metabolism, *Freshwater Biol.*, *46*, 1503–1517.
- Mulholland, P. J., J. N. Houser, and K. O. Maloney (2005), Stream diurnal dissolved oxygen profiles as indicators of in-stream metabolism and disturbance effects: Fort Benning as a case study, *Ecol. Indicators*, *5*, 243–252.
- Müllner, A. N., and M. Schagerl (2003), Abundance and vertical distribution of the phytobenthic community within a pool and riffle sequence of an alpine gravel stream, *Int. Rev. Hydrobiol.*, *88*, 243–254.
- O'Connor, B. L., M. Hondzo, D. Dobraca, T. M. LaPara, J. C. Finlay, and P. L. Brezonik (2006), Quantity-activity relationship of denitrifying bacteria and environmental scaling in streams of a forested watershed, *J. Geophys. Res.*, *111*, G04014, doi:10.1029/2006JG000254.
- Odum, H. T. (1956), Primary production in flowing waters, *Limnol. Oceanogr.*, *1*, 102–117.
- Opsahl, R. W., T. Welnitz, and N. L. Poff (2003), Current velocity and invertebrate grazing regulates stream algae: Results of an in situ electrical exclusion, *Hydrobiologia*, *499*, 135–145.
- Owens, M., R. Edwards, and J. Gibbs (1964), Some reaeration studies in streams, *Int. J. Air Water Pollut.*, *8*, 469–486.
- Petts, G. E. (2000), A perspective on the abiotic processes sustaining the ecological integrity of running waters, *Hydrobiologia*, *422/423*, 15–27.
- Potter, M. C., D. C. Wiggert, M. Hondzo, and T. I. P. Shih (2002), *Mechanics of Fluids*, 3rd ed., Brooks/Cole, Pacific Grove, Calif.
- Power, M. E. (1984), Habitat quality and the distribution of algae-grazing catfish in a Panamanian stream, *J. Animal Ecol.*, *53*, 357–374.
- Power, M. E. (1990), Benthic turfs versus floating mats of algae in river food webs, *Oikos*, *58*, 67–79.
- Power, M. E., N. Brozovic, C. Bode, and D. Zilberman (2005), Spatially explicit tools for understanding and sustaining inland water ecosystems, *Frontiers Ecol. Environ.*, *3*, 47–55.
- Rounick, J. S., and S. V. Gregory (1981), Temporal changes in periphyton standing crop during an unusually dry winter in streams of the western Cascades, Oregon, *Hydrobiologia*, *83*, 197–205.
- Southwood, T. R. E. (1977), Habitat: The template for ecological strategies?, *J. Animal Ecol.*, *46*, 337–365.
- SPSS Inc. (2001), SPSS for Windows, release 11.0.1, Chicago, Ill.
- Tal, M., K. Gran, A. B. Murray, C. Paola, and D. M. Hicks (2004), Riparian vegetation as a primary control on channel characteristics in multi-thread rivers, in *Riparian Vegetation and Fluvial Geomorphology*, *Water Sci. Appl. Ser.*, vol. 8, edited by S. J. Bennett and A. Simon, pp. 43–58, AGU, Washington, D. C.
- Townsend, S. A., and A. Padovan (2005), The seasonal accrual and loss of benthic algae (Spirogyra) in the Daily River, an oligotrophic river in tropical Australia, *Mar. Freshwater Res.*, *56*, 317–327.
- Trudeau, V., and J. B. Rasmussen (2003), The effect of water velocity on stable carbon and nitrogen isotope signatures of periphyton, *Limnol. Oceanogr.*, *48*, 2194–2199.
- Uehlinger, U., C. König, and P. Reichert (2000), Variability of photosynthesis—Irradiance curves and ecosystem respiration in a small river, *Freshwater Biol.*, *44*, 493–507.
- Vannote, R. L., G. W. Minshall, K. W. Cummins, J. R. Sedell, and C. E. Cushing (1980), The river continuum concept, *Can. J. Fish. Aquat. Sci.*, *37*, 130–137.
- Wang, H., M. Hondzo, C. Xu, V. Poole, and A. Spacie (2003), Dissolved oxygen dynamics of streams draining an urbanized and agricultural catchment, *Ecol. Modell.*, *160*, 145–161.
- Webster, I. T., N. Rea, A. V. Padovan, and P. Dostine (2005), An analysis of primary production in the Daily River, a relatively unimpacted tropical river in northern Australia, *Mar. Freshwater Res.*, *56*, 303–316.
- Welnitz, T., and R. B. Rader (2003), Mechanisms influencing community composition and succession in mountain stream periphyton: Interactions between scouring history, grazing, and irradiance, *J. N. Am. Benthol. Soc.*, *22*, 528–541.
- Whitford, L. A., and G. J. Schumacher (1964), Effect of current on respiration and mineral uptake in *Spirogyra* and *Oedogonium*, *Ecology*, *45*, 168–170.
- Wootton, J., M. S. Parker, and M. E. Power (1996), Effects of disturbance on river food webs, *Science*, *273*, 1558–1560.
- Young, R. G., C. R. Townsend, and C. D. Matthaei (2004), Functional indicators of river ecosystem health—An interim guide for use in New Zealand, *Cawthron Rep.* 870, 54 pp., Minist. for the Environ., Nelson, New Zealand.

M. Hondzo and T. A. Warnars, Saint Anthony Falls Laboratory, Department of Civil Engineering, University of Minnesota, Mississippi River at 3rd Ave. SE, Minneapolis, MN 55414-2196, USA. (mhondzo@umn.edu)

M. E. Power, Department of Integrative Biology, University of California, 4184 Valley Life Sciences Bldg., Berkeley, CA 94720, USA.